Supporting Information

$OvoA_{Mtht}$ in *Methyloversatilis thermotolerans* ovothiol biosynthesis is a bifunctional enzyme: cysteine dioxygenase and sulfoxide synthase activities

Ronghai Cheng,[a†] Andrew C. Weitz,[a†] Jared Paris,[b†] Yijie Tang,[b] Jingyu Zhang,[c] Heng Song,[a] Nathchar Naowarojna,[a] Kelin Li,[a] Lu Qiao,[a] Juan Lopez,[a] Mark W. Grinstaff,[a] Lixin Zhang,[c] Yisong Guo,[b*] Sean Elliott,[a*] Pinghua Liu[a*]

[a] R. Cheng, A. Weitz, H. Song, N. Naowarojna, L. Qiao, J. Lopez, K. Li, M. Grinstaff, Prof. S. Elliott, and Prof. P. Liu, Department of Chemistry, Boston University, 590 Commonwealth Ave., Boston, MA 02215
E-mail: elliott@bu.edu, pinghua@bu.edu
[b] J. Paris, Y. Tang, and Prof. Y. Guo, Department of Chemistry, Carnegie Mellon University, 4400 Fifth Avenue, Pittsburgh, PA 15213
E-mail: ysguo@andrew.cmu.edu
[c] Jingyu Zhang, and Prof. Lixin Zhang, State Key Laboratory of Bioreactor Engineering, East China University of Science and Technology, 130 Meilong Rd, Shanghai, 200237, China, E-mail: lxzhang@ecust.edu.cn
[†] These authors contributed equally to this work

Table of content

Materials and methods.

Histidine and cysteine from Sigma-Aldrich. Hercynine was synthesized from previously published protocol.[1,2] Proton nuclear magnetic resonance spectra were recorded using Agilent 500 (500 MHz VNMRS). Chelex-100 resin was purchased from Bio-Rad laboratory. The Iron content was quantified by Agilent MP AES atomic emission spectroscopy. Reaction products were analyzed by LC−MS on a LTQ-FT-ICR mass spectrometer (Thermo Scientific).

Bioinformatics analysis of $OvoA_{Mtht}$

The protein coding sequences of strains with "thermo" keywords were downloaded from the ftp server of NCBI taxonomy database. There were 122 strains found in total. Protein sequence of OvoA from *Erwinia tasmaniensis* (accession number: WP_012439783.1) and EgtB from *Mycobacterium thermoresistibile* (accession number: WP_050811957.1) were then used as the query sequences for protein blast analysis with E value of 10^{-10}. The all-to-all blast was performed on all OvoA- or EgtB-homologs with E value of 10^{-20} and 10^{-60} to construct protein similarity network. The protein similarity network was then visualized by Cytoscape 3.8.2. The protein domain analysis was perform using the Pfam program.

Protein overexpression and purification.

Cell growth and heterologous expression of ^{56}Fe-loaded $OvoA_{Mtht}$ in *Escherichia coli*

$OvoA_{Mtht}$ gene (accession number: WP_018410809.1) was codon-optimized for *Escherichia coli* overexpression by Genscript. The gene sequence sub-cloned to pASK-IBA3plus vector. Competent cell BL21(DE3) was transformed with the plasmid and a single colony was inoculated into 50 mL LB media supplemented with 50 µg/mL kanamycin at 37 °C overnight. Then, 10-mL of seed culture was used to inoculate 1 L of LB media supplemented with 100 µg/mL amplicillin at 37 °C. When OD_{600} reached 0.6-0.8, protein overexpression was induced with anhydrous tetracycline to 0.5 mg/L final concentration. The protein was overexpressed at 25 °C for 14 hours. The cell was collected by centrifugation.

Purification of ^{56}Fe-loaded $OvoA_{Mtht}$ and its variants

30 g cell was resuspended in 150 ml 100 mM Tris-HCl, 500 mM NaCl, 10% glycerol, pH = 8.0 buffer. 150 mg lysozyme was added and the mixture was incubated on ice for 30 minutes. After sonication, $(NH_4)_2Fe(SO_4)_2$ was added to 0.15 mM final concentration and ascorbate was added to 0.3 mM final concentration. Cell debris was removed by centrifugation at 19500 rpm for 45 minutes. The target protein was then purified by following the same protocol as reported for $OvoA_{Eta}$ and concentrated to around 80 mg/ml.[2]

Preparation of iron-free LB media by chelex-100 cation exchange resin

After 75 g LB broth was dissolved in 1.5 L distilled water, the mixture was treated with 300 ml of chelex-100 resin (sodium form) to remove metal ions. The metal ion depleted medium was then supplemented with 3 ml of 1000x trace element stock solution (20 mM $CaCl_2$, 20 mM $MnCl_2$, 2 mM $CoCl_2$, 10 mM Zn_2SO_4, 2 mM $CuCl_2$, 100 mM $MgCl_2$, 2 mM $(NH_4)_2Mo_2$, 2 mM $CuCl_2$ in distilled water). The pH of the media was adjusted to 7.2 by 10 M NaOH solution and the final volume was adjusted to 3 L. The iron content of the medium was quantified by atomic emission spectroscopy. The medium was then autoclaved for the production of the desired [^{57}Fe]-labeled $OvoA_{Mtht}$.

Cell growth and heterologous expression of ^{57}Fe-loaded $OvoA_{Mtht}$ in *Escherichia coli*

Competent cell BL21(DE3) was transformed with the plasmid and a single colony was inoculated into 50 mL LB media supplemented with 100 µg/mL ampicillin at 37 °C overnight. Then, 10-mL of seed culture was used to inoculate 1 L of iron-free media supplemented with 100 µg/mL amplicillin and 0.01 mM $^{57}FeCl_2$ (it was prepared by dissolving ^{57}Fe in 0.6 M HCl solution) at 37 °C. 5g of glucose was added for as a carbon source. When OD_{600} reached 0.6-0.8, protein

overexpression was induced with anhydrous tetracycline to a final concentration 0.5 mg/L. After additional 14 hours at 25 °C, cells were collected by centrifugation.

Purification of ^{57}Fe-loaded $OvoA_{Mtht}$ and its variants

30 g of cell was dissolved in 150 ml 100 mM Tris-HCl, 500 mM NaCl, 10% glycerol, pH = 8.0 buffer. 150 mg lysozyme was added and the mixture was incubated on ice for 30 minutes. After sonication. $^{57}FeCl_2$ was added to a final concentration of 0.15 mM and ascorbate was added to a final concentration 0.3 mM. Cell debris was removed by centrifugation at 19500 rpm for 45 minutes. The [^{57}Fe]-labeled $OvoA_{Mtht}$ was then purified using a protocol similar to the ^{56}Fe-containing $OvoA_{Mtht}$ in the previous section and concentrated to a concentration of 80 mg/ml. The protein concentration was quantified by amino acid analysis.

Iron content quantification of $OvoA_{Mth}$

10 µL of 1.4 mM $OvoA_{Mth}$ was diluted by adding 990 µL 2 % (w/w) HNO_3. The protein precipitates were removed by centrifugation at 16000 rpm for 10 minutes. The iron standard (0.125 ppm to 2 pm) was made by dilution of 1000 ppm iron standard stock solution by 2 % (w/w) HNO_3. The supernatant was taken and analyzed by atomic emission spectroscopy. The sample uptake time was 15 s and stabilization time was 10 s. The emission spectrum at 371.993 mm was recorded for iron concentration quantification. The calibration curve was made from iron standards above. The iron content was calculated based on the protein concentration, iron concentration and sample dilution factor.

^{1}H-NMR assay of $OvoA_{Mtht}$ when histidine analogs and cysteine were used as the substrates.

A typical 1-ml reaction contained 2 µM $OvoA_{Mtht}$, 1 mM histidine or its analog (monomethyl histidine, dimethyl histidine and hercynine), 1 mM cysteine, 1 mM tris(2-carboxyethyl) phosphine (TCEP), 0.2 mM sodium ascorbate in 50 mM potassium phosphate buffer, pH 8.0. The reaction was stirred at 25 °C for 30 minutes and the protein was then removed by ultrafiltration. The filtrate was lyophilized and dissolved in 350 µL D_2O for ^{1}H-NMR analysis.

^{13}C-NMR analysis of $OvoA_{Mtht}$ using [β-^{13}C]-cysteine as the substrate.

A typical 1-ml reaction contained 20 µM $OvoA_{Mtht}$, 1 mM histidine or derivatives (monomethyl histidine, dimethyl histidine and hercynine), 1 mM [β-^{13}C]-cysteine, 1 mM tris(2-carboxyethyl) phosphine (TCEP), 0.2 mM sodium ascorbate in 50 mM potassium phosphate buffer, pH 8.0. The protein from the reaction mixture was removed by ultrafiltration. The filtrate was lyophilized and dissolved in 350 µL D_2O and analyzed by ^{13}C-NMR.

Steady state kinetics of $OvoA_{Mtht}$ using histidine and cysteine as substrates.

Histidine concentration dependence

A typical 1-ml reaction contained 0.17 µM $OvoA_{Mtht}$, variable concentration of histidine (0.25 mM to 8 mM), 10 mM cysteine, 2 mM tris(2-carboxyethyl) phosphine (TCEP), 0.2 mM sodium ascorbate in 50 mM potassium phosphate buffer, pH 8.0. The overall oxygen consumption rate was monitored using the NeoFoxy oxygen electrode.

Cysteine concentration dependence

A typical 1-ml reaction contained 0.17 µM $OvoA_{Mtht}$, variable concentration of cysteine (0.75 mM to 4 mM), 10 mM histidine, 2 mM tris(2-carboxyethyl) phosphine (TCEP), 0.2 mM sodium ascorbate in 50 mM potassium phosphate buffer, pH 8.0. The overall oxygen consumption rate was monitored bythe NeoFoxy oxygen electrode.

Steady state kinetics of $OvoA_{Mtht}$ using hercynine and cysteine

Hercynine concentration dependence

A typical 1-ml reaction contained 0.6 μM $OvoA_{Mtht}$, variable concentration of hercynine (0.1 mM to 6 mM), 10 mM cysteine, 2 mM tris(2-carboxyethyl) phosphine (TCEP), 0.2 mM sodium ascorbate in 50 mM potassium phosphate buffer, pH 8.0. The overall oxygen consumption rate was monitored by the NeoFoxy oxygen electrode.

Cysteine concentration dependence

A typical 1-ml reaction contained 0.43 μM $OvoA_{Mtht}$, variable concentration of cysteine (0.5 mM to 10 mM), 10 mM hercynine, 2 mM tris(2-carboxyethyl) phosphine (TCEP), 0.2 mM sodium ascorbate in 50 mM potassium phosphate buffer, pH 8.0. The overall oxygen consumption rate was monitored by the NeoFoxy oxygen electrode.

Steady state kinetics of $OvoA_{Mtht}$ using cysteine as the only substrate.

A typical 1-ml reaction contained 2.7 μM $OvoA_{Mtht}$, variable concentration of cysteine (1 mM to 125 mM), 2 mM tris(2-carboxyethyl) phosphine (TCEP), 0.2 mM sodium ascorbate in 50 mM potassium phosphate buffer, pH 8.0. The overall oxygen consumption rate was monitored by the NeoFoxy oxygen electrode.

Steady state kinetics of $OvoA_{Mtht,Y405F}$ using histidine and cysteine as the substrates.

Hercynine concentration dependence

A typical 1-ml reaction contained 0.27 μM $OvoA_{Mtht,Y405F}$, variable concentration of hercynine (0.05 mM to 5 mM), 10 mM cysteine, 2 mM tris(2-carboxyethyl) phosphine (TCEP), 0.2 mM sodium ascorbate in 50 mM potassium phosphate buffer, pH 8.0. The overall oxygen consumption rate was monitored by the NeoFoxy oxygen electrode.

Cysteine concentration dependence

A typical 1-ml reaction contained 0.27 μM $OvoA_{Mtht,Y405F}$, variable concentration of cysteine (0.05 mM to 5 mM), 10 mM hercynine, 2 mM tris(2-carboxyethyl) phosphine (TCEP), 0.2 mM sodium ascorbate in 50 mM potassium phosphate buffer, pH 8.0. The overall oxygen consumption rate was monitored by the NeoFoxy oxygen electrode.

Mössbauer Analysis

The Mössbauer samples were prepared by mixing ^{57}Fe-loaded $OvoA_{Mtht}$ (90% ^{57}Fe loading) in anoxic buffer solution (100 mM Tris-HCl, 500 mM NaCl, 10% glycerol, pH 8.0) with cysteine, histidine, or both in the same buffer solution. The mixtures were loaded into in-house made plastic Mössbauer cups and incubated for 5 minutes before frozen. All procedures were conducted in a MBraun glovebox filled with N_2 gas, the O_2 level was maintained at < 0.5 ppm. The final concentrations of various reagents are: [$OvoA_{Mtht}$] = 0.7 mM, [His] = 25 mM, [Cys] = 25 mM. Mössbauer spectra were recorded with home-built spectrometers using Janis Research SuperVaritemp dewars, which allowed studies in the temperature range from 1.5 to 200 K, and applied magnetic fields up to 8.0 T. Mössbauer spectra simulations were performed using the WMOSS software package (SEE Co., Edina, MN). Isomer shifts are quoted relative to Fe metal at 298 K. All Mössbauer figures were prepared using SpinCount software.[3]

Preparation of NO-bound $OvoA_{Mtht}$ complexes for EPR analysis.

Standardization of PROLI-NONOate stock solutions

All samples were prepared in a Coy Laboratories anaerobic chamber. First, PROLI-NONOate (Cayman Chemical Company) stock solutions were prepared and standardized following a previously established methodology.[4] Briefly, approximately 10 mg PROLI-NONOate were dissolved in 1 mL of deoxygenated 10 mM NaOH on the same day of EPR sample preparation. The NO delivery equivalents of the PROLI-NONOate stock solution was standardized by the reaction of the generated NO with Fe^{II}EDTA at pH 7. A 50 mM stock solution of $Fe(NH_4)(SO_4)_2$•$6H_2O$ was prepared fresh, and mixed 1:1 (v/v) with 100 mM EDTA at pH 7. 10 μL PROLI-NONOate solution was mixed with 490 μL of 50 mM HEPES pH 7.0, followed approx.

60 s later by addition of 500 µL of the EDTA stock solution. The resultant mixture was quantified by measuring the absorbance at 440 nm of the Fe^{II}EDTA-NO complex (ϵ_{440nm} = 900 $M^{-1}cm^{-1}$). With the stock solution of PROLI-NONOate standardized, an appropriate volume of stock PROLI-NONOate was diluted in 10 mM NaOH to prepare 1 mL of 5 mM NO(g) equivalents. This solution was used for preparation of the EPR samples.

Preparation of EPR samples

A typical 250 µL reaction mixture contained 100 µM $OvoA_{Mtht}$, 200 µM NO(g), 0.5 mM ascorbate, and variable Cysteine or Histidine in the sample buffer (100 mM Tris-HCl, pH 8.0 buffer with 50 mM NaCl). Working stock solutions of ~1 mM $OVOA_{Mtht}$, 10 mM cysteine, 10 mM histidine, and 100 mM sodium ascorbate were diluted appropriately in the sample buffer. First, the protein was diluted with approximately 100 µL sample buffer, and pre-incubated with substrate and ascorbate for before adding the PROLI-NONOate. Before adding to the enzyme-substrate mixture, 10 µL of the PROLI-NONOate stock solution (containing 5 mM NO(g) equivalents) was first diluted into approximately 100 µL sample buffer before mixing this resultant solution with the enzyme-substrate mixture. The final mixture was incubated for 5 minutes and then transferred into an EPR sample tube. The samples were flash frozen in liquid nitrogen for EPR analysis. We found empirically that pre-incubating enzyme and substrate before adding NO, and diluting the NONOate first into buffer before mixing with enzyme minimized protein degradation and reaction byproducts. In the ascorbate-free samples, an appropriate volume of additional buffer was provided to replace the missing ascorbate. In the 10% (v/v) glycerol-containing samples, the sample buffer was pre-mixed with anaerobic glycerol before adding enzyme or substrate.

EPR Spectroscopy

X-Band EPR spectra were collected on a Bruker ELEXYS-II E500 EPR spectrometer equipped with a helium continuous flow cryostat model ESR 900 (Oxford Instruments, Inc.). Temperature was controlled with an Oxford Instruments ITC 503 Digital Cryogenic temperature controller. Unless otherwise noted, all spectra were recorded using the following standard parameters: modulation frequency, 100 kHz; modulation amplitude, 10 G; conversion time, 100 ms; time constant 3.6 ms; microwave frequency 9.38 GHz. Microwave power and sample temperature were adjusted to ensure spectra were collected at nonsaturating conditions (listed in figure captions). EPR signals were quantified relative to a 2.78 mM Cu^{II}EDTA standard at pH 4.0 in 10% (v/v) glycerol. The Cu^{II} of known concentration was from a commercially-certified AAS standard solution in 2% nitric acid (Sigma Aldrich).

Quantitative spectral simulations were performed using the software SpinCount developed by M.P. Hendrich.[3] The simulations were calculated with least-squares fitting using the spin Hamiltonian:

$$H = \beta \mathbf{B}\cdot\mathbf{g}\cdot\mathbf{S} + D[S_z^2 - S(S+1)/3 + (E/D)(S_x^2 - S_y^2)],$$

Where D and E are the axial and rhombic zero-field splitting parameters, and B represents the applied magnetic field.

Results and discussion

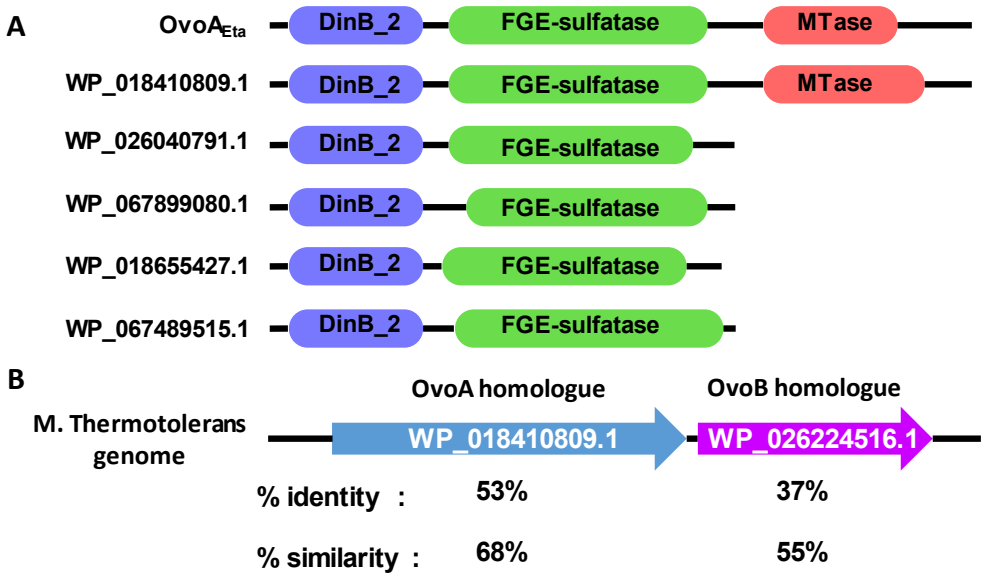

Figure S1. Protein domain analysis and gene neighborhood analysis of five candidate genes from the protein similarity network.
(A) Protein domain organization of the five candidate proteins. All of them had the DinB_2 iron binding domain and FGE-sulfatase domain, which are necessary for EgtB sulfoxide synthase activity. However, one of the candidates, WP_018410809.1 from *Methyloversatilis thermotolerans*, has an additional methyltransferase domain (Pfam name: Methyltransf_31). Both Egt1 and OvoA have the methyltransferase domain;[5, 6] **(B)** Gene neighborhood analysis of WP_018410809.1 in *Methyloversatilis thermotolerans* genome revealed that there is an OvoB homolog with more than 50% similarity with OvoB from *Erwinia tasmaniensis*.

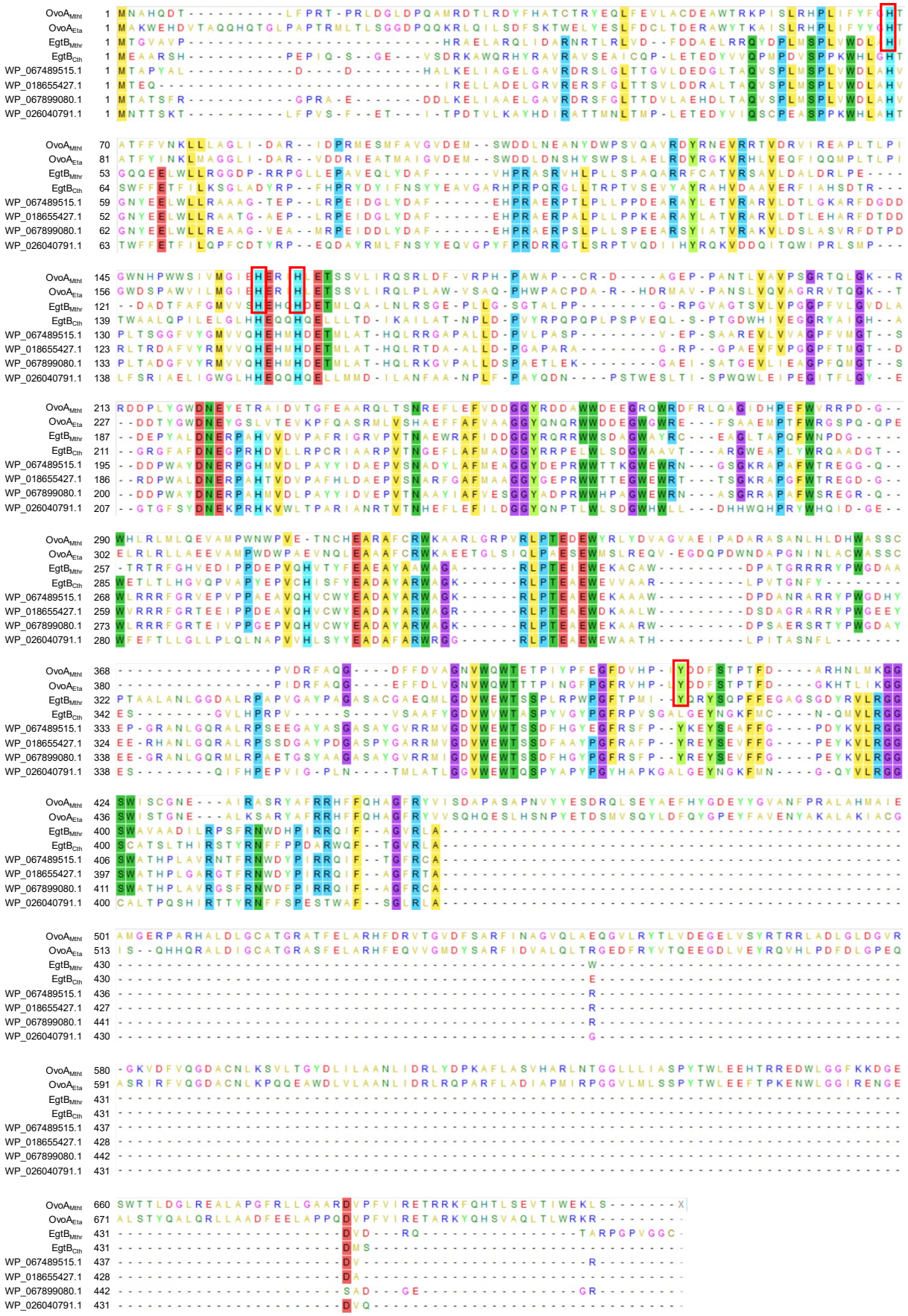

Figure S2. Multiple sequence alignment of OvoA$_{Eta}$, EgtB$_{Mthr}$, EgtB$_{Cth}$ and five putative OvoA thermostable candidates.

Based on the sequence alignment results, most of them have the three conserved histidine residues for iron coordination and a conserved tyrosine that might be important for controlling the partitioning between CDO and sulfoxide synthase activities (Y417 in OvoA$_{Eta}$ and Y405 in

$OvoA_{Mtht}$). These key residues are highlighted in the red boxes. However, only $OvoA_{Mtht}$ has the methyltransferase domain compared to others four candidates.

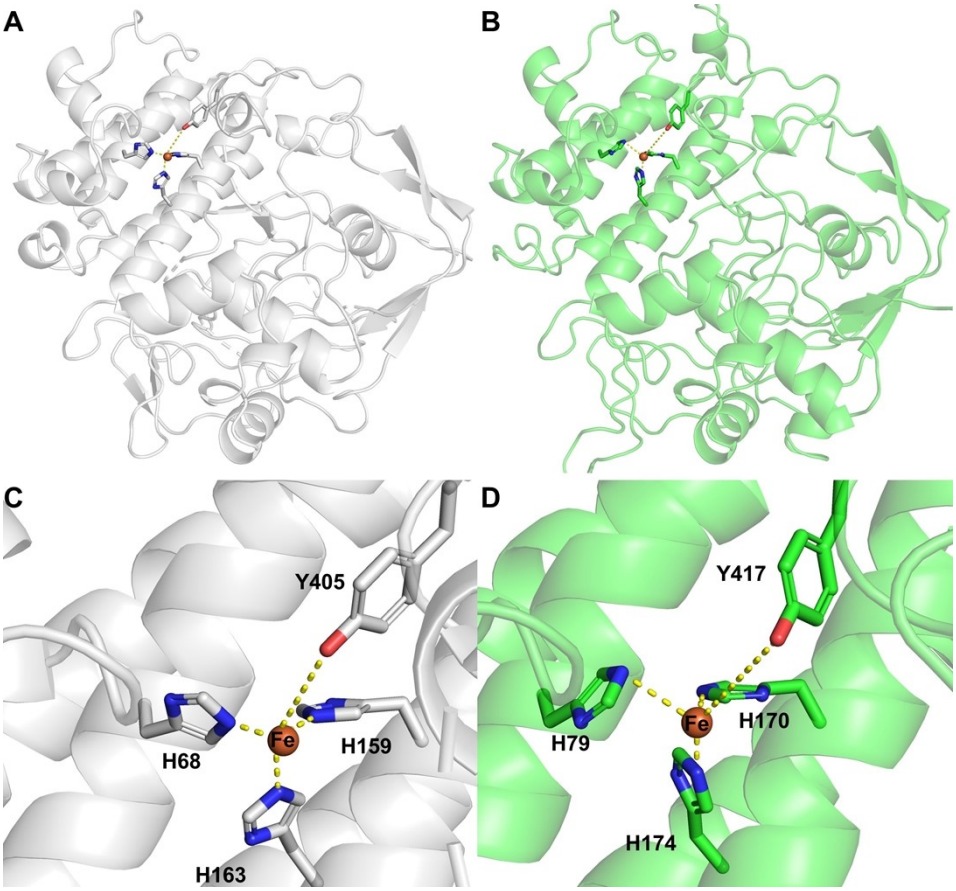

Figure S3. Comparison of $OvoA_{Mtht}$ and $OvoA_{Eta}$ structure models predicted by Phyre2 program.[7]

(A) Overall structure model of $OvoA_{Mtht}$. **(B)** Overall structure model of $OvoA_{Eta}$. **(C)** Zoom-in view of proposed iron active site of $OvoA_{Mtht}$ structure model. **(D)** Zoom-in view of proposed iron active site of $OvoA_{Eta}$ structure model. In $OvoA_{Mtht}$, H68, H159 and H163 are predicted to be the iron ligands and Y405 is predicted to be an active site tyrosine residue. Both the overall structure and active site enviroment in $OvoA_{Eta}$ and $OvoA_{Mtht}$ are similar, indicating that $OvoA_{Mtht}$ might be an ovothiol biosynthetic enzyme. The structure model was built based on $EgtB_{Mthr}$ structure (PDB code: 4X8B)

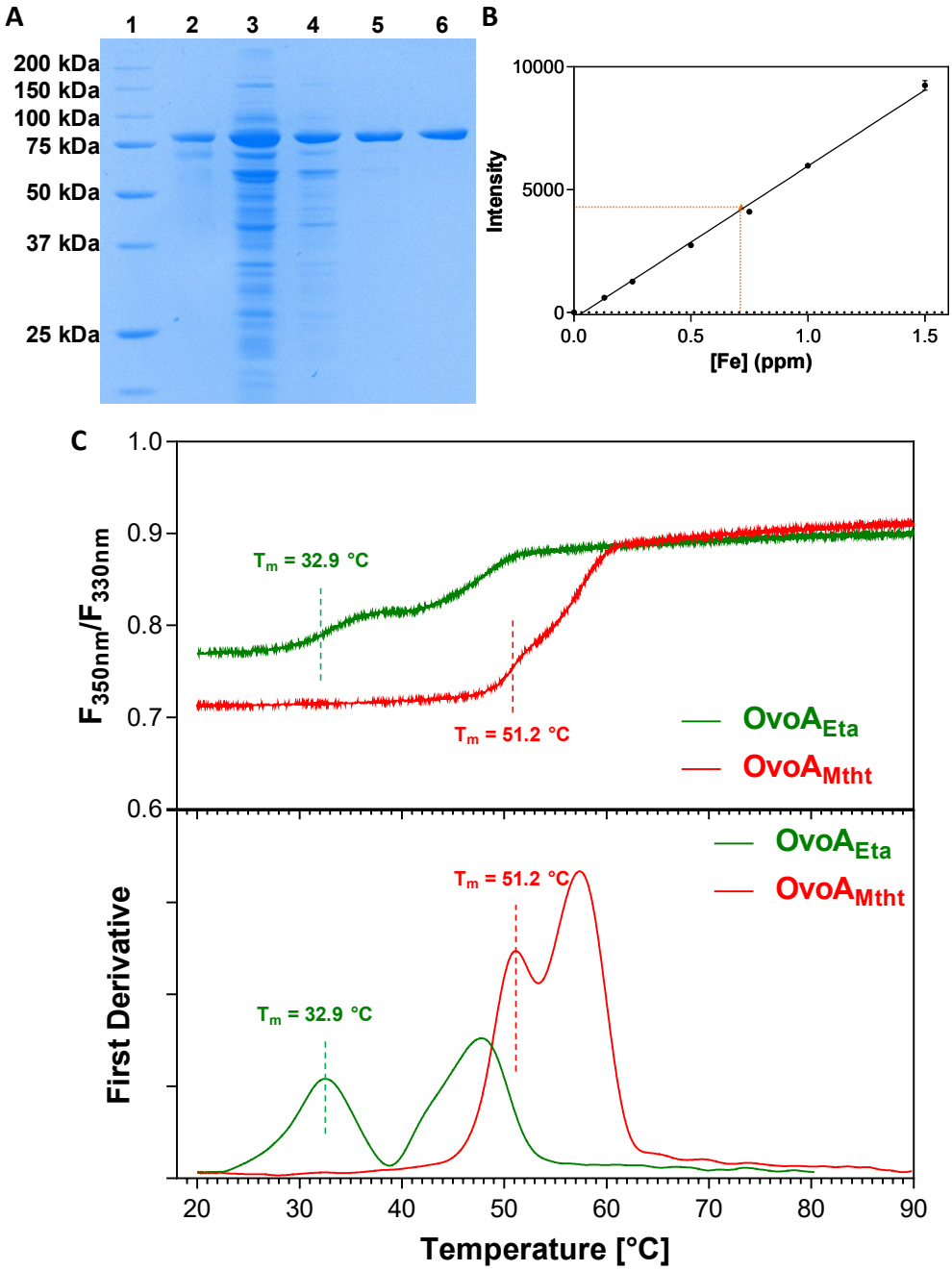

Figure S4. Biochemical characterization of $OvoA_{Mtht}$.
(A) SDS-PAGE analysis of the anaerobic $OvoA_{Mtht}$ purification samples. Lane 1: protein marker; lane 2: in-house OvoA protein standard; lane 3: supernatant; lane 4: a flow-through fraction; 5: a washing fraction; lane 6: an elution fraction. **(B)** Iron content quantification of $OvoA_{Mtht}$. The orange dot was the measured iron content from the sample during the assay for 13 µM of $OvoA_{Mtht}$ protein. **(C)** Thermo unfolding curves of $OvoA_{Mtht}$ and $OvoA_{Eta}$ by nanoDSF assay. Changes in the F350/F330 fluorescence ratio (top) and the corresponding first derivative (bottom) were shown. The sample was composed of 10 µg protein in 20 mM Tris-HCl, pH 8.0 buffer. The nanoDSF parameters were: 20 °C to 90 °C with rate of 1 °C/min. The T_m was calculated based on the 1st inflection point of F_{350nm}/F_{330n} ratio's 1st derivative. The experiment was repeated twice to confirm the accuracy of T_m measurement.

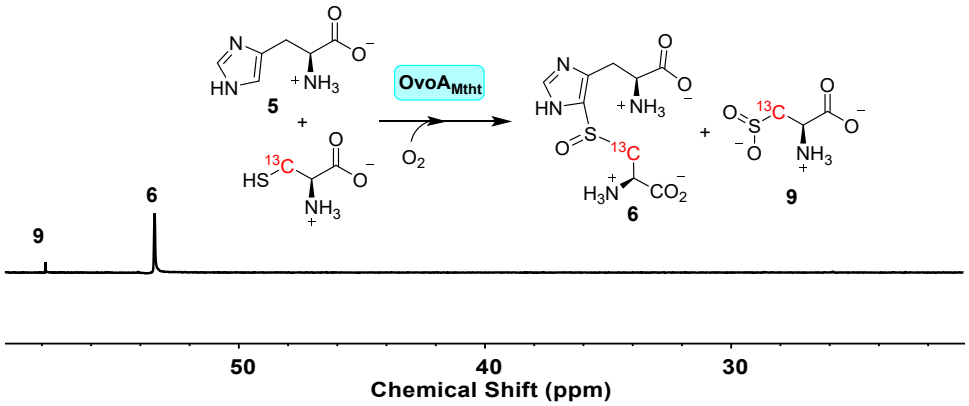

Figure S5. ^{13}**C-NMR analysis of OvoA$_{Mtht}$ reactions using [β-^{13}C]-cysteine and histidine as the substrates**.

The signal at 53 ppm is from the [^{13}C]-labeled sulfoxide **6**. The signal at 58 ppm is from [β-^{13}C]-cysteine sulfinic acid. In this reaction, sulfoxide **6** is the major product (90%) and cysteine sulfinic acid is the minor product (10%).

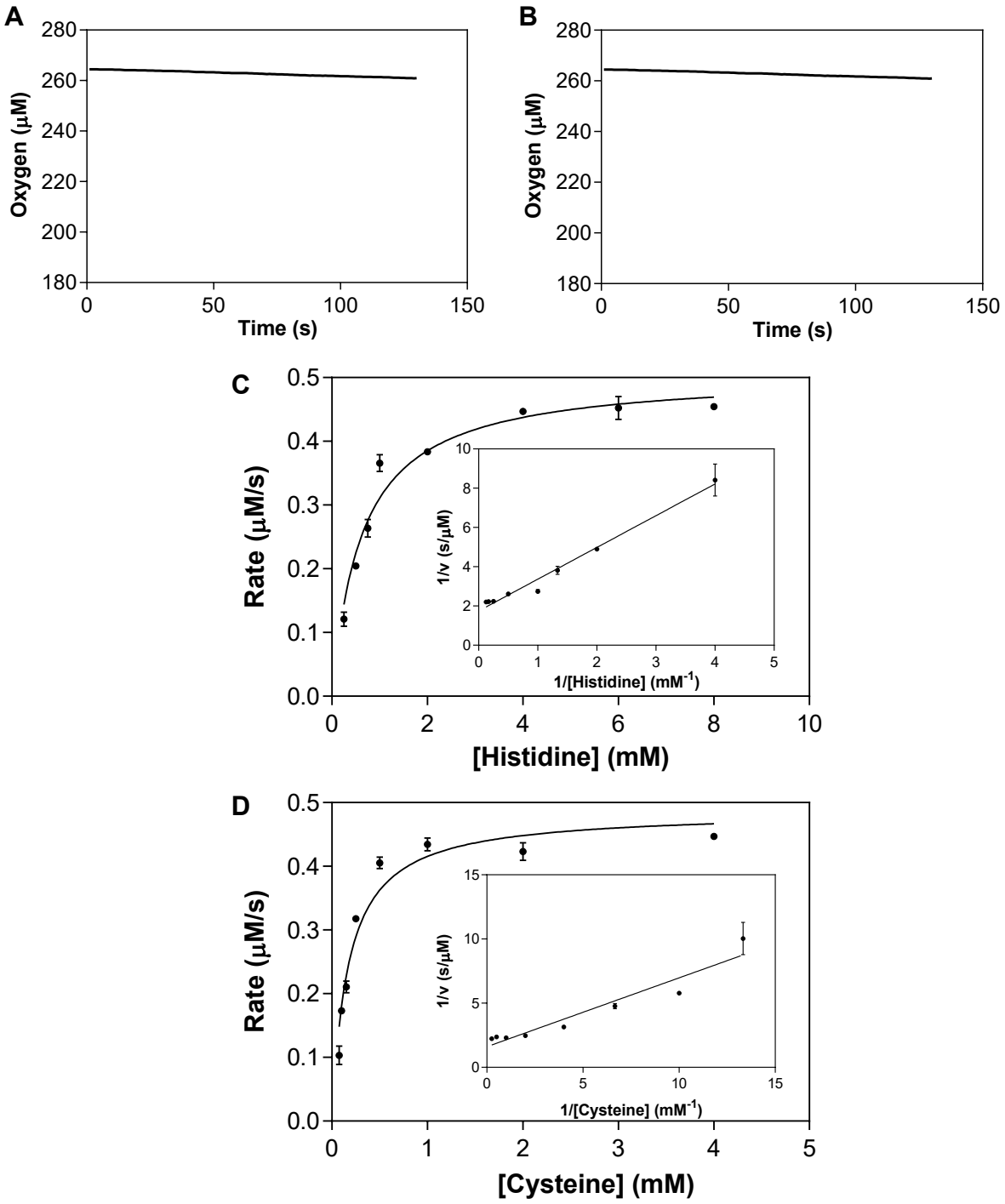

Figure S6. Steady-state kinetics of $OvoA_{Mtht}$ using cysteine and histidine as the substrates. **(A)** oxygen consumption trace of a reaction mixture with 50 mM cysteine, 2 mM TCEP, 0.2 mM sodium ascorbate, in 50 mM potassium phosphate buffer pH 8.0. It monitored the oxygen consumption caused by reductants auto-oxidation. **(B)** oxygen consumption trace of a reaction with 2 μM $OvoA_{Mtht}$, 2 mM TCEP, 0.2 mM sodium ascorbate in 50 mM potassium phosphate buffer, pH 8.0, It monitored the oxygen consumption caused by uncoupled oxygen consumption. The reaction rate was calculated by the slope of each trace. The reaction rate caused by uncoupled oxygen consumption and reductant auto-oxidation was 0.023 μM/s and 0.021 μM/s, respectively **(C)** histidine concentration dependence; **(D)** cysteine concentration dependence; The reaction rate was measured by monitoring the overall oxygen consumption rate. The kinetics parameters are: $k_{cat,O2}$ = 168.8±4.5 min^{-1}; $K_{M,\,his}$ = 630.1 ± 63.6 μM and $K_{M,\,cys}$ = 171.6 ± 18.6 μM.

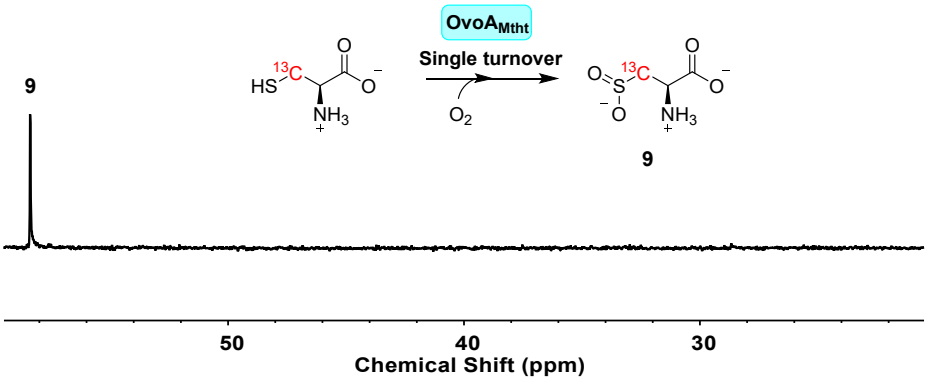

Figure S7. ^{13}C-NMR analysis of OvoA$_{Mtht}$ single-turnover reaction using only [β-^{13}C]-cysteine as the substrate.

The 1.5 mL reaction composed of 400 μM OvoA$_{Mtht}$, 360 μM [β-^{13}C]-cysteine in 50 mM potassium phosphate buffer pH 8.0 was setup under O_2 atmosphere at room temperature. After the reaction, the protein was quenched by chloroform and the protein precipitates were removed by centrifugation. The supernatant was lyophilized, dissolved in D_2O and analyzed by ^{13}C-NMR, which indicated that cysteine sulnific acid is the only product in this reaction.

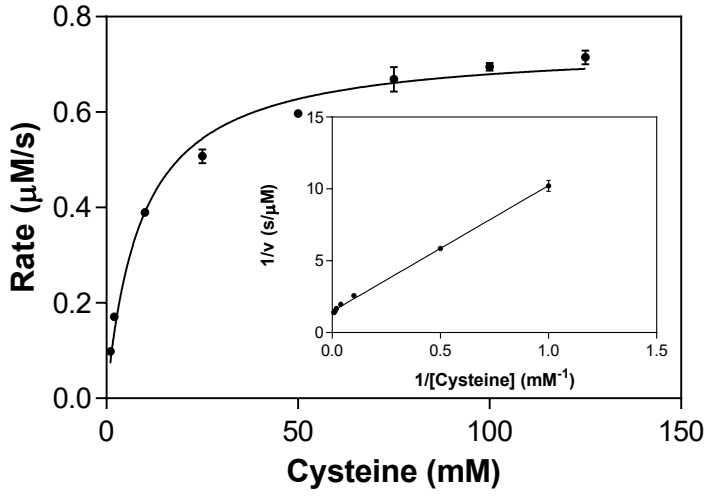

Figure S8. Steady-state kinetics of OvoA$_{Mtht}$ using cysteine as the only substrate.

The reaction rate was measured by monitoring the overall oxygen consumption rate. The kinetics parameters are: $k_{cat,O2}$ = 16.2±0.2 min^{-1} and $K_{M,\ cys}$ = 8.1 ± 0.6 mM.

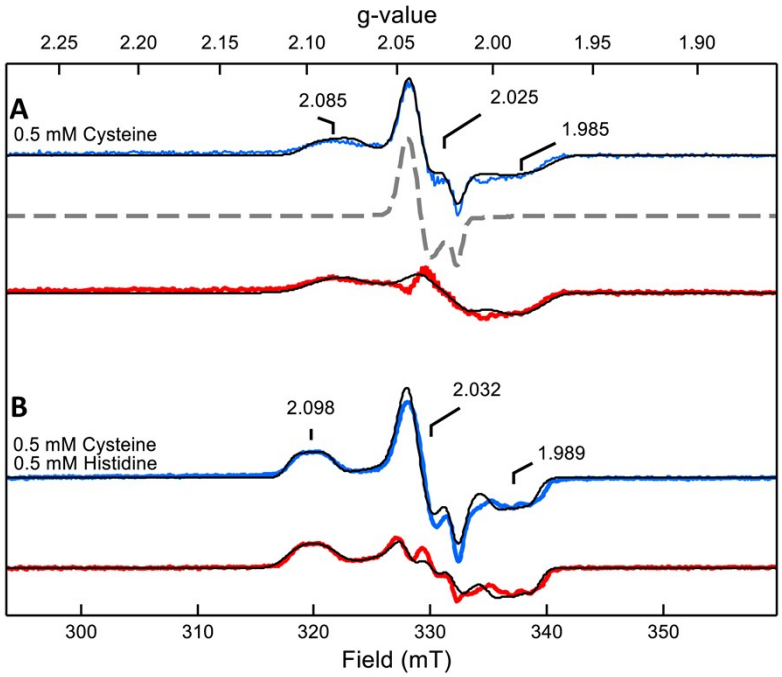

Figure S9. X-band EPR spectra of the *g* ~2 region of of NO treated substrate-$OvoA_{Mtht}$ complexes.
(A) 0.1 mM $OvoA_{Mtht}$ pre-incubated with 0.5 mM cysteine prior to addition of 0.2 mM NO(g). **(B)** 0.1 mM $OvoA_{Mtht}$ pre-incubated with 0.5 mM cysteine and 0.5 mM histidine prior to addition of 0.2 mM NO(g). In blue are the raw data, and in red are the spectra following subtraction of the DNIC signal (grey dashed line). The black traces are quantitative simulations of the corresponding data. Overlaid the blue spectra is a sum of simulation for both the S = ½ $\{FeNO\}^7$ species and the DNIC species. Overlaid the red spectra is just the simulation for the S = ½ $\{FeNO\}^7$ species. Simulation parameters given in **Table S3**. EPR spectra collected at 15 K, a modulation amplitude of 0.5 mT, and a microwave power of 63 μW.

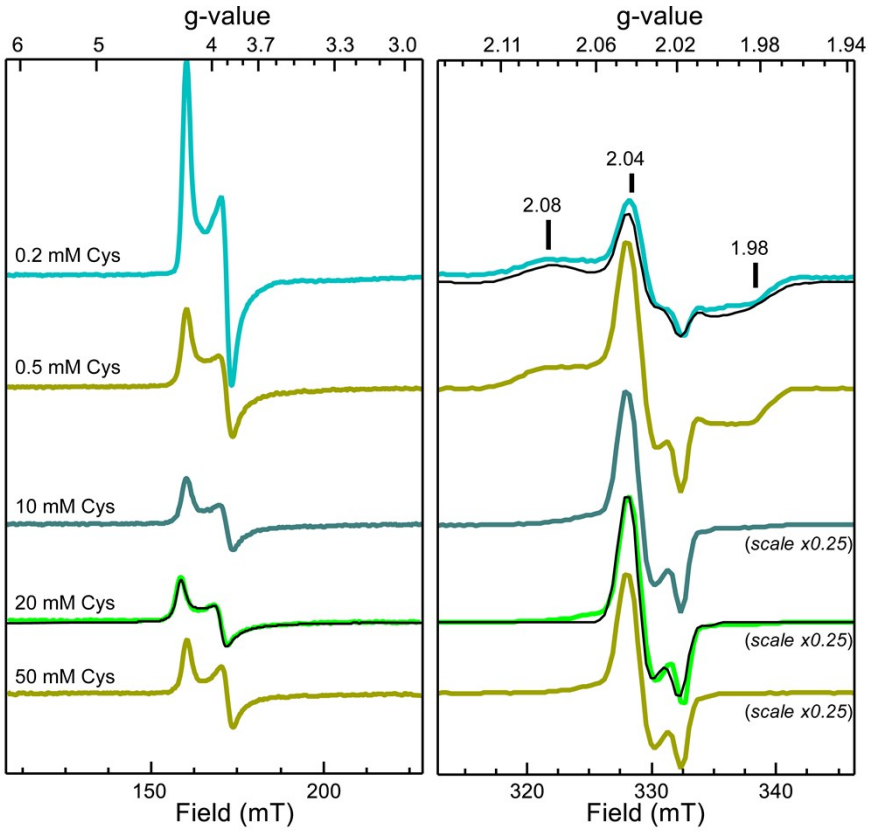

Figure S10. X-band EPR spectra of NO treated cysteine•OvoA$_{Mtht}$ complexes.
(Left Panel) Low field region of spectra showing $S = 3/2$ $\{FeNO\}^7$ species near $g \sim 4$ region. (Right Panel) High field region showing mixtures of the purported $S = ½$ $\{FeNO\}^7$ species and the dinitrosyl impurity species. The signals corresponding to the same [Cys] shown in the two panels are from the same recorded EPR spectrum. Except when otherwise noted, the signal intensity scaling between the left and right panels are identical. No other signals were detectable between applied fields of 0 – 500 mT. Conditions: T = 15 K; microwave power = 63 μW, modulation amplitude = 1 mT.

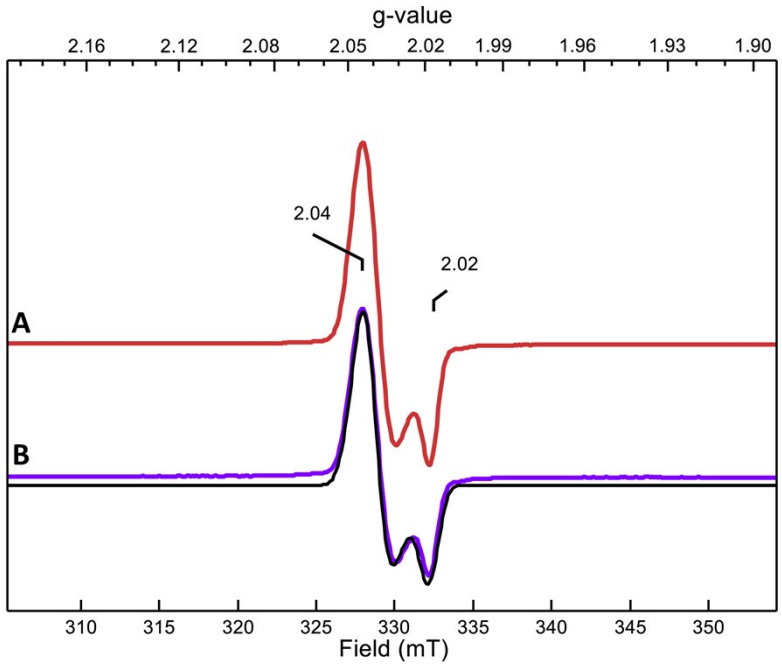

Figure S11. EPR spectra of iron dinitrosyl complex formed by mixing iron, cysteine/histidine, and NO in the absence of protein.
(A) 0.1 mM Fe, 0.5mM Cysteine, 0.2 mM NO; **(B)** 0.1 mM Fe, 0.5 mM Cysteine, 0.5 mM Histidine, 0.2 mM NO. The black trace is a simulation of spectrum A of a S = ½ species with g = (2.041, 2.041, 2.01), with g-strain σg = (0.005, 0.005, 0.002) (values represent one standard deviation of a normal Gaussian distribution). EPR spectra collected at 15 K and a microwave power of 63 μW.

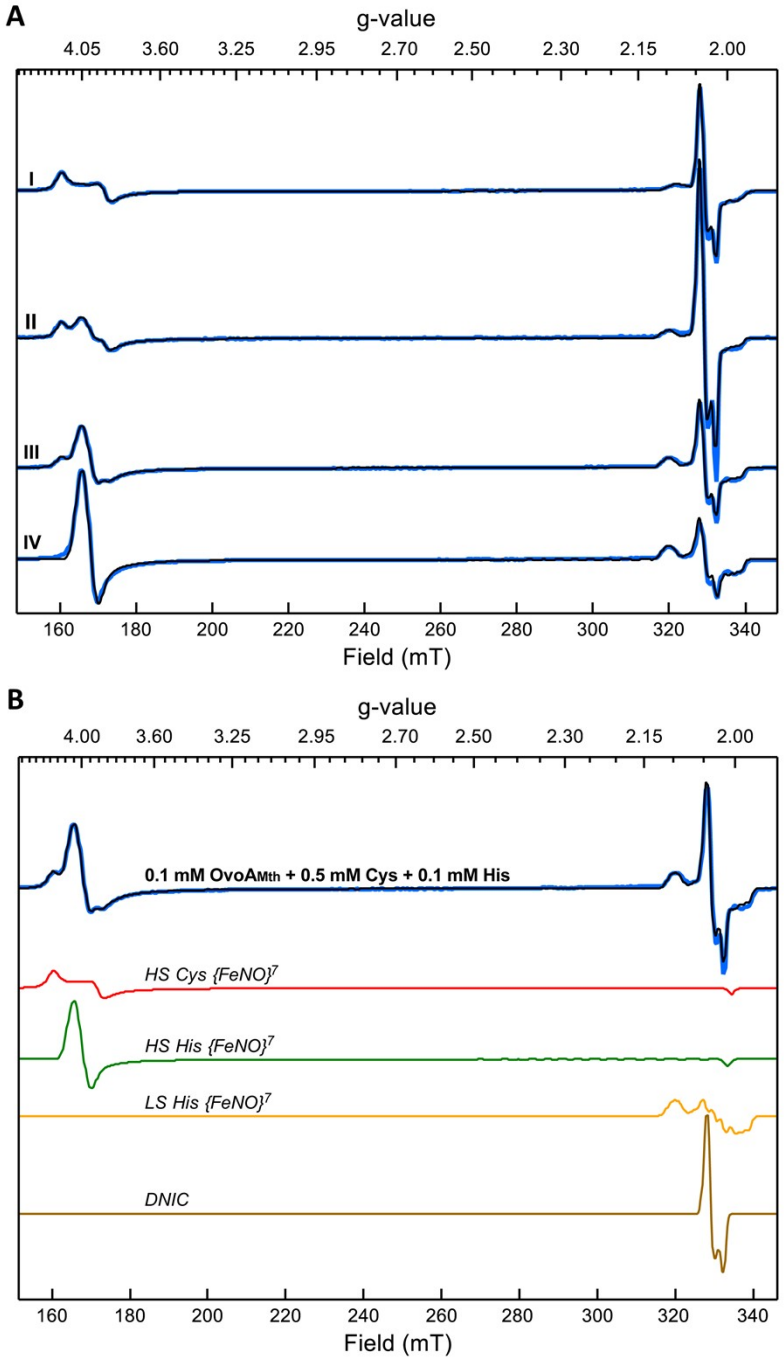

Figure S12. Histidine concentration dependence of EPR signal.
(A) X-Band EPR spectra at 15 K of 0.1mM $OvoA_{Mtht}$ with varying amounts of histidine along with 0.5 mM cysteine prior to addition of 0.2 mM NO from PROLI-NONOate. I) 0 mM His; II) 0.05 mM His; III) 0.1 mM His; (IV) 0.5 mM His. In blue are the experimental spectra, overlaid with black traces representing quantitative simulations of the sum of species listed in **Table S3**. **(B)** As an example, the spectrum of 0.1 mM $OvoA_{Mtht}$ mixed with 0.5 mM Cys, 0.1 mM His, and 0.2 mM NO is shown (III), with a deconvolution of the individual species used to generate the

simulations seen in Panel A. The "Cys $\{FeNO\}^7$" and "His $\{FeNO\}^7$" labels refer to the $\{FeNO\}^7$ species associated with either the addition of Cysteine only or Histidine + Cysteine, respectively. Experimental Conditions: Temperature = 15 K, microwave power = 63 µW, modulation frequency = 1 mT.

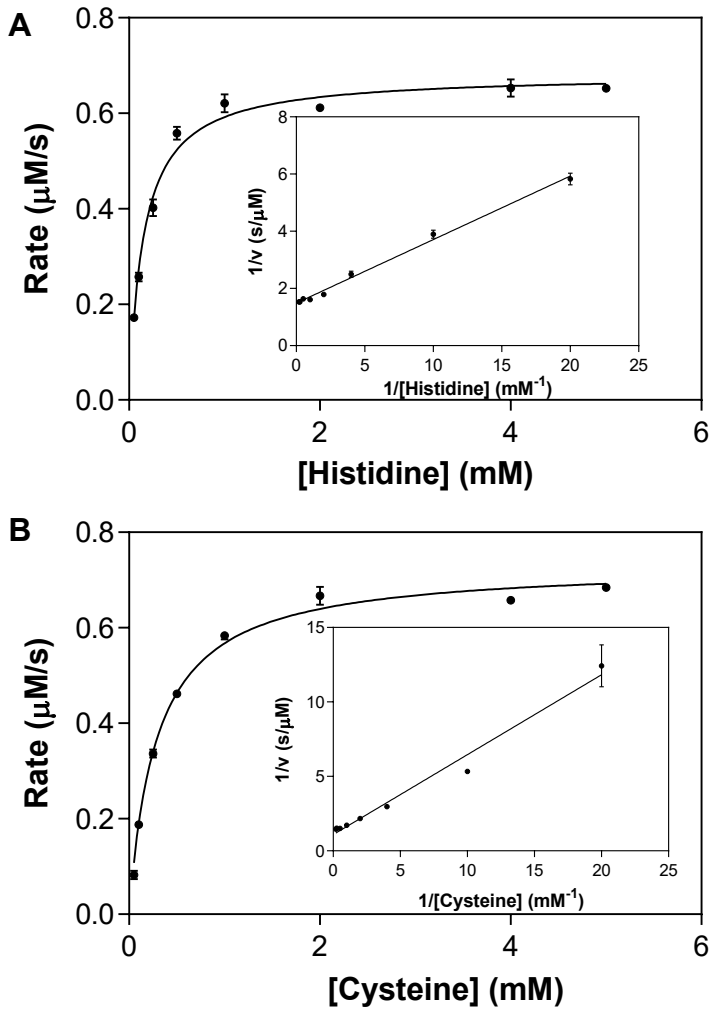

Figure S13. Steady-state kinetics of $OvoA_{Mtht,Y405F}$ using cysteine and histidine as the substrates.
The reaction rate was measured by monitoring the overall oxygen consumption rate. The kinetics parameters are: $k_{cat,O2}$ = 162.6±2.1 min^{-1}; $K_{M,\,his}$ = 152.4 ± 11.0 µM and $K_{M,\,cys}$ = 290.0 ± 16.1 µM.

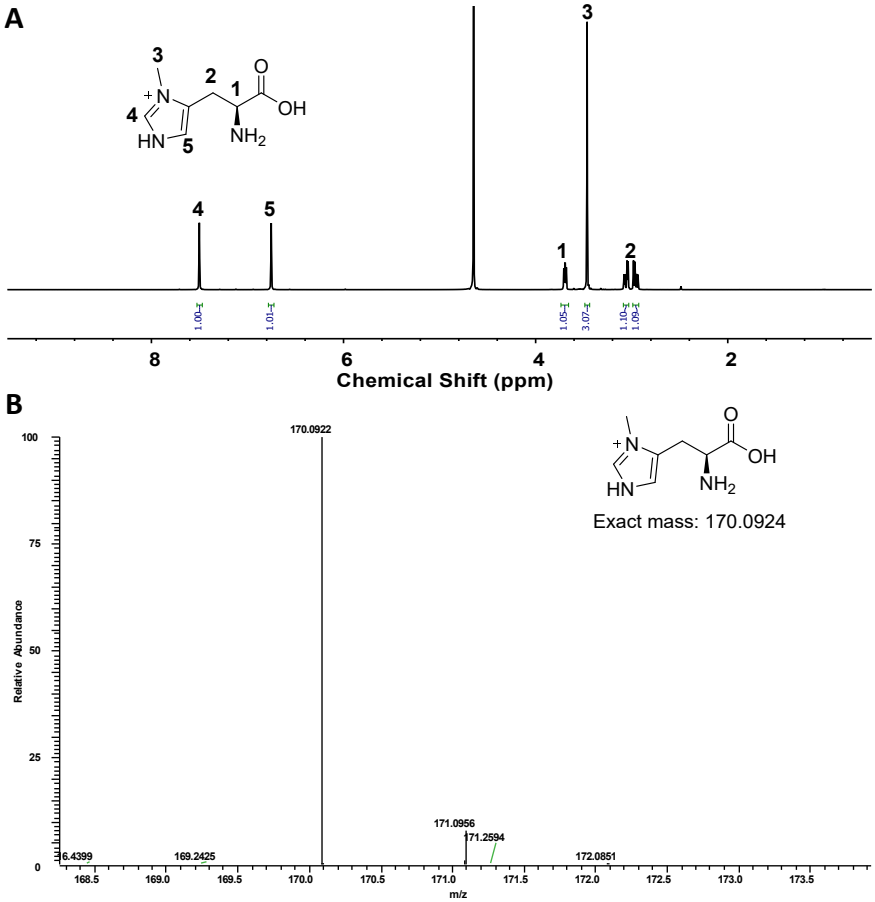

Figure S14. Characterization of π-*N*-methyl-histidine.
(A) ^{1}H NMR (500 MHz, deuterium oxide) δ 7.50 (s, 1H), 6.75 (s, 1H), 3.69 (dd, J = 7.8, 5.5 Hz, 1H), 3.46 (s, 3H), 3.06 (dd, J = 16.0, 5.5 Hz, 1H), 2.96 (dd, J = 16.0, 7.8 Hz, 1H). **(B)** MS spectrum of π-*N*-methyl-histidine. Calculated *m*/*z* ratio for π-*N*-methyl-histidine ($[M+H]^+$ form, positive mode) was 170.0924 and found at 170.0922.

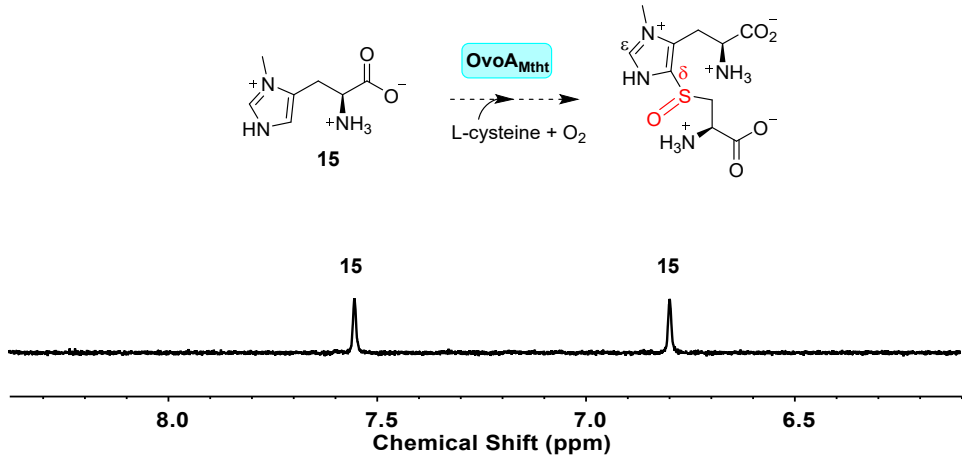

Figure S15. ^{1}H-NMR analysis of $OvoA_{Mtht}$ sulfoxide synthase regioselectivity using π-*N*-methyl-histidine and cysteine as the substrates.
There is no detectable sulfoxide product formation (~ 7.8 ppm).

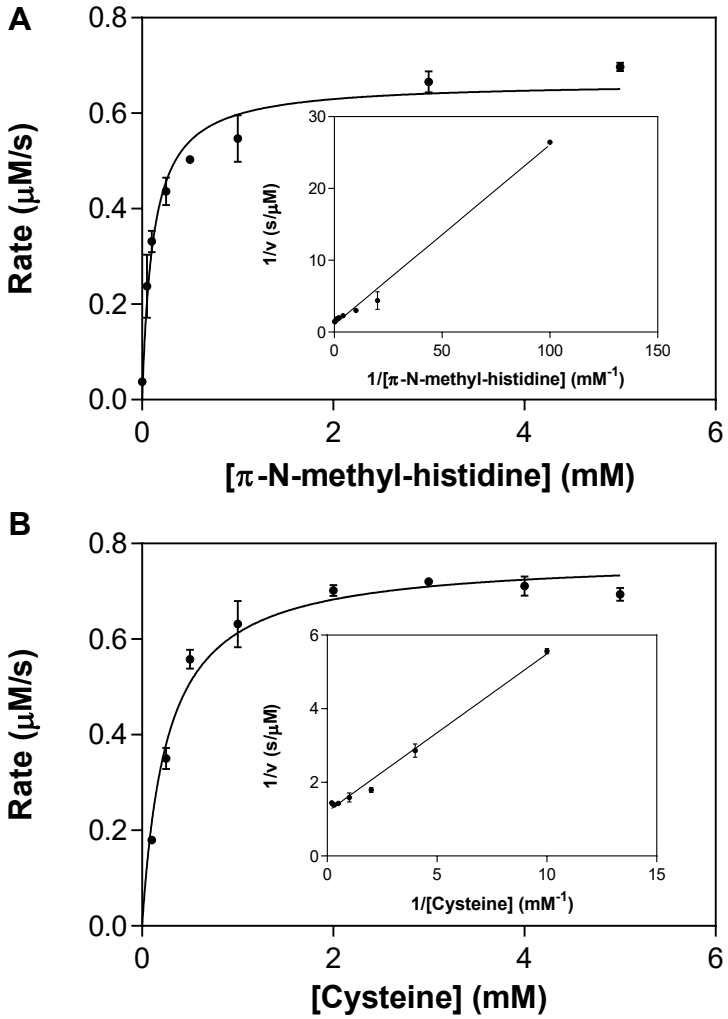

Figure S16. Steady-state kinetics of $OvoA_{Mtht}$ using cysteine and **π-*N*-methyl-histidine as the substrates**.

(A) π-*N*-Methyl-histidine concentration dependence; **(B)** Cysteine concentration dependence. The reaction rate was measured by monitoring the overall oxygen consumption rate. The kinetics parameters are: $k_{cat,O2}$ = 99.2 ± 2.7 min^{-1}; $K_{M,\pi\text{-N-methyl-histidine}}$ = 112.2 ± 17.4 μM and $K_{M,\,cys}$ = 249.1 ± 28.3 μM.

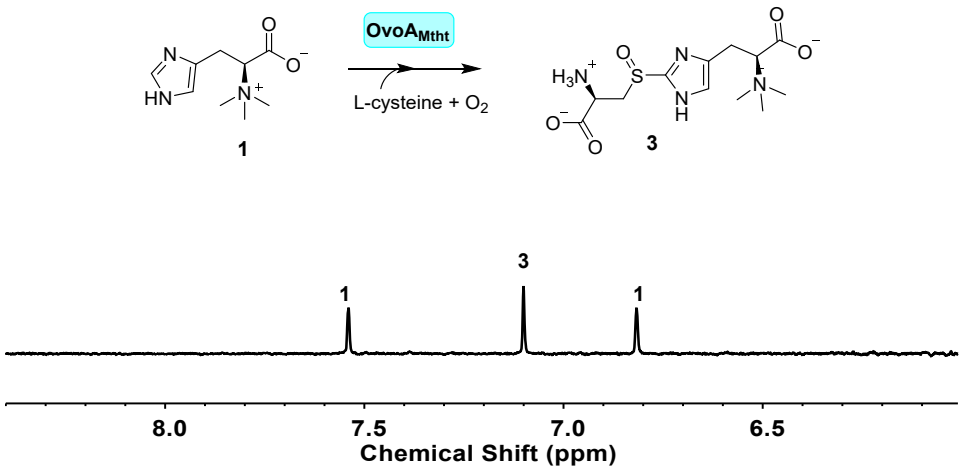

Figure S17. ^{1}H-NMR analysis of OvoA$_{Mtht}$ sulfoxide synthase regioselectivity using hercynine and cysteine as the substrates.
The signal at ~ 7.1 ppm represent the imidazole ε-H atom from the sulfoxide **3**. The other two signals are from hercynine imidazole H-atoms.

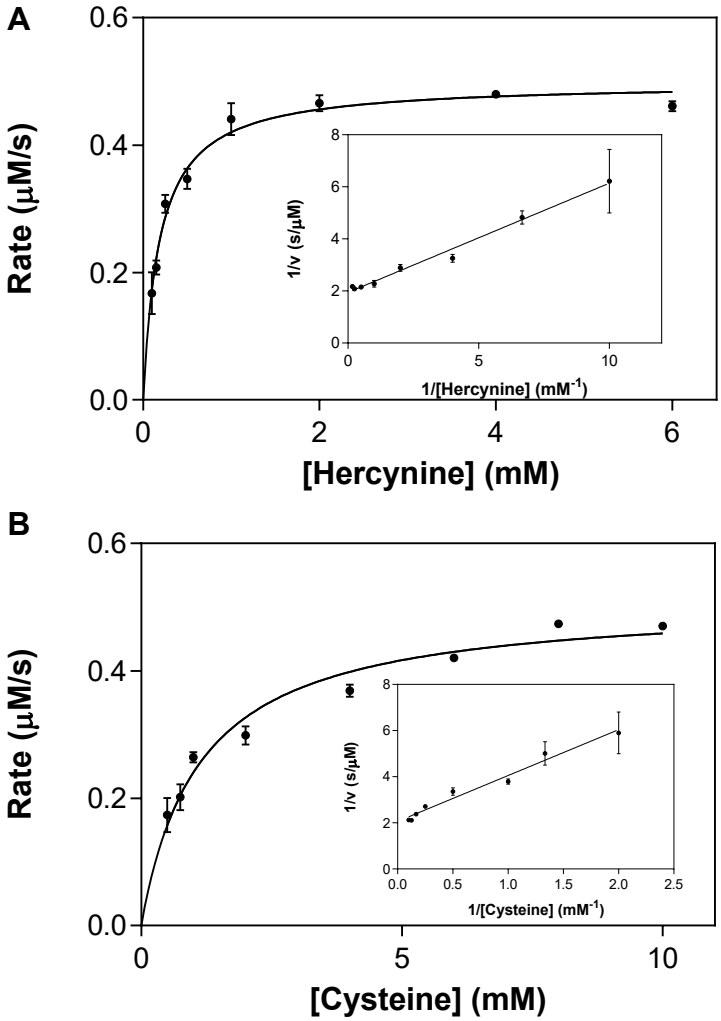

Figure S18. Steady-state kinetics of OvoA$_{Mtht}$ using cysteine and hercynine as the substrates.
(A) Hercynine concentration dependence kinetics. **(B)** Cysteine concentration dependence kinetics. The reaction rate was measured by monitoring the overall oxygen consumption rate. The kinetics parameters are: $k_{cat,O2}$ = 47.8±4.2 min^{-1}; $K_{M,\ hercynine}$ = 185.9 ± 17.2 μM and $K_{M,\ cys}$ = 1060.2 ± 121.2 μM.

Table S1. Mössbauer simulation parameters for the $OvoA_{Mtht}$ Mössbauer spectra.

	Species	δ (mm/s)	ΔE_Q (mm/s)	Linewidth (mm/s)	Relative Area (%)
Fe(II)-OvoA	A	1.22	2.25	0.40	40
	B	1.25	2.80	0.40	60
OvoA+His	A	1.22	2.25	0.40	28
	B	1.25	2.80	0.40	40
	C	1.24	3.13	0.29	21
Fe(II)-OvoA+Cys	A	1.22	2.25	0.40	6
	B	1.25	2.80	0.40	17
	D	1.158	3.364	0.325	75
OvoA+Cys+His	E	1.17	3.12	0.40	92

Table S2. Concentrations of iron nitrosyl complexes in cysteine to $OvoA_{Mtht}$ titration experiment

	HS $\{FeNO\}^7$	LS $\{FeNO\}^7$	dinitrosyl
0.2 mM Cys	100 µM	7 µM	1.4 µM
0.5 mM Cys	52 µM	9 µM	4 µM
10 mM Cys	31 µM	9 µM	20 µM
20 mM Cys	27 µM	-	20 µM
50 mM Cys	26 µM	-	20 µM

Table S3. Simulation parameters of the *S* = 1/2 species in Figure S9

Species	g_x, g_y, g_z	$\sigma g_{x,y,z}$	A_x, A_y, A_z	LW (mT)
$[L_2Fe(NO)_2]^9$	2.042,2.042,2.0418	0.005,0.005,0.002	-	1.0
$\{FeNO\}^7$, Cys	2.085,2.025,1.985	0.01,-,0.005	40,40,40	0.5
$\{FeNO\}^7$, Cys + His	2.098,2.032,1.989	-	40,55,40	0.73

Table S4: Yield of species as a function of histidine concentration

	HS Cys $\{FeNO\}^7$	LS Cys $\{FeNO\}^7$	HS His $\{FeNO\}^7$	LS His $\{FeNO\}^7$	DNIC
0 mM His	54 µM (73%)	11 µM (15%)	-	-	8 µM (12%)
0.05 mM His	47 µM (55%)	n.d.[1]	13 µM (15%)	11 µM (13%)	15 µM (17%)
0.1 mM His	33 µM (39%)	n.d.[1]	32 µM (38%)	14 µM (17%)	5 µM(6%)
0.5 mM His	n.d.[1]	n.d.[1]	75 µM (77%)	19 µM (20%)	3 µM (3%)

[1]It is possible to simulate a small amount of this species (5 µM or less) to fit the data, but the resolution of the data is not sufficient to conclusively establish its presence in the data.

Supporting discussion

Previous reports on CDO-like enzymes have suggested that excess Cysteine may have a detrimental effect in the yield of {FeNO}^{7} complex formation.[8] Accordingly, we initially prepared a titration series where $OvoA_{Mtht}$ was incubated with varying cysteine concentrations prior to NO addition, to determine the best substrate conditions to monitor the formed {FeNO}^{7} complexes. The results of this experiment are in **Figure S10**. The best yield of the high spin $S = 3/2$ {FeNO}^{7} species was when 0.2 mM cysteine were incubated with 0.1 mM $OvoA_{Mtht}$ (or 2 equivalents relative to the enzyme). In this sample, there was approximately quantitative formation of the $S = 3/2$ {FeNO}^{7} species. Quantitative simulations showed that this species accounted for 0.1 mM {FeNO}^{7}. In the $g \sim 2$ region (right panel), there were also trace amounts of the low spin {FeNO}^{7} species at g = 2.08 and 1.98 (7 μM), and the dinitrosyl byproduct at g = 2.04 (2 μM). A full table of the species observed and their concentrations as determined by simulations for this titration series is provided in **Table S2**.

As discussed in the main text, in the high field $g \sim 2$ region, there were predominantly two signals found when $OvoA_{Mtht}$ was incubated with cysteine, histidine, and NO. First, the signal at $g = 2.04$ was characterized as a dinitrosyl iron complex byproduct (DNIC), $[L_2Fe(NO)_2]$[9], commonly present when adding NO(g) to non heme iron enzymes. As a control, samples of 0.1 mM free Fe^{II} were mixed with PROLI-NONOate (0.2 mM NO delivered) and either 0.5 mM cysteine or 0.5 mM histidine + 0.5 mM cysteine, and frozen in an EPR tube. The X-Band EPR spectra of these samples are shown in **Figure S11**. The data show that under these conditions, the DNIC is reproduced in the absence of protein. Furthermore, histidine addition appears to have no effect on the signal.

With the $g = 2.04$ species identified as a DNIC byproduct, the spectral features of the $S = ½$ {FeNO}^{7} species were studied next. While this species was present in only a minority amount (< 10%), this preliminary data indicates similar spectral properties with the low spin {Fe(ES)-NO}^{7} species observed with bidenate bound Cysteine in CDO. Between repeated batches of similar samples, the amount of the DNIC impurity could be minimized, but never fully eliminated. Simulations to model the {FeNO}^{7} species were then performed on data with the DNIC signal subtracted, shown in **Figure S9**. In the cysteine-only sample (**Figure S9A**), the low spin species had *g*-values of 2.085, 2.025, and 2.01. The data were simulated with an isotropic ^{14}N ($I = 1$) hyperfine splitting of 40 MHz. This value is within the range of hyperfine interactions from NO bound to other non heme iron complexes in a $S = ½$ configuration.[9] While the triplet pattern commonly observed at g_y for CDO and MDO is absent,[10] it is possible that this feature cannot be well-resolved owing to its low yield and the DNIC background signal. Still, the simulation suggests that assignment of this species as a low spin form of the Cys-bound {FeNO}^{7} complex observed in MDO and CDO is at least *plausible*. More work needs to be done to determine the factors that influence its relative yield vs the high spin species in $OvoA_{Mtht}$, to draw further comparisons to the Cys-bound {FeNO}^{7} species found in CDO and MDO.

When histidine is added with cysteine to the enzyme prior to NO incubation, the g-values of the low spin species shift slightly more rhombic, to 2.098, 2.032, and 1.989. In this case, following subtraction of the DNIC signal, there appears to be a triplet pattern at g_y. Simulations were fit to the data using ^{14}N hyperfine values of $A_x = A_z = 40$ MHz, and $A_y = 55$ MHz. These hyperfine values are also in reasonable agreement with those observed in CDO and MDO, but because this species constitutes a minority of the sample (< 10 %), further comparisons of the low spin species with these enzymes is beyond the scope of this discussion.

Reference

1. K. N. White and J. P. Konopelski, *Org. Lett.*, 2005, **7**, 4111-4112.
2. H. Song, M. Leninger, N. Lee and P. Liu, *Org. Lett.*, 2013, **15**, 4854-4857.
3. D. T. Petasis and M. P. Hendrich, *Meth. Enzymol.*, 2015, **563**, 171-208.
4. J. D. Caranto, A. Weitz, M. P. Hendrich and D. M. Kurtz, *J. Am. Chem. Soc.*, 2014, **136**, 7981-7992.
5. W. Hu, H. Song, A. Sae Her, D. W. Bak, N. Naowarojna, S. J. Elliott, L. Qin, X. Chen and P. Liu, *Org. Lett.*, 2014, **16**, 5382-5385.
6. N. Naowarojna, P. Huang, Y. Cai, H. Song, L. Wu, R. Cheng, Y. Li, S. Wang, H. Lyu, L. Zhang, J. Zhou and P. Liu, *Org. Lett.*, 2018, **20**, 5427-5430.
7. L. A. Kelley, S. Mezulis, C. M. Yates, M. N. Wass and M. J. E. Sternberg, *Nat. Protoc.*, 2015, **10**, 845-858.
8. B. S. Pierce, B. P. Subedi, S. Sardar and J. K. Crowell, *Biochemistry*, 2015, **54**, 7477-7490.
9. B. S. Pierce, J. D. Gardner, L. J. Bailey, T. C. Brunold and B. G. Fox, *Biochemistry*, 2007, **46**, 8569-8578.
10. S. Sardar, A. Weitz, M. P. Hendrich and B. S. Pierce, *Biochemistry*, 2019, **58**, 5135-5150.